Electronic supplementary information for:

Ruthenium complexes featuring cooperative phosphine-pyridine-iminophosphorane (PNN) ligands: synthesis, reactivity and catalytic activity.

Thibault Cheisson, Louis Mazaud, and Audrey Auffrant,*

LCM, CNRS-Ecole polytechnique, Université Paris-Saclay, F-91128 Palaiseau Cedex

audrey.auffrant@polytechnique.edu

Table of contents

I. X-Ray Crystallography

Table S1 : Crystallographic Data for [$\mathbf{L^{Cy}}$.LiCl]$_2$, [$\mathbf{L^{Cy}}$.LiCl.THF], $\mathbf{1^{Ph}}$

	[L^{Cy}.LiCl]$_2$	**L^{Cy}.LiCl.THF**	**1^{Ph}**
Formula	$C_{74}H_{100}Cl_2Li_2N_4P_4$	$C_{41}H_{58}ClLiN_2OP_2$	$C_{61}H_{53}Cl_2N_2P_3Ru$
Mw	1254.23	699.22	1078.93
Space group	P 2_1/c	P -1	P2_1/c
V (Å^3)	3484.4(4)	3914.3(5)	5180.4(6)
a (Å)	10.437(1)	11.582(1)	18.448(1)
b (Å)	16.826(1)	15.915(1)	10.888(1)
c (Å)	19.843(1)	22.595(1)	26.346(1)
α (deg)	90	109.675(1)	90.00
β (deg)	90.720(1)	92.224(1)	101.784(1)
γ (deg)	90	91.818(1)	90.00
Z	2	4	4
d (g.cm^{-3})	1.195	1.186	1.383
F(000)	1344	1504	2544
θ_{max}	25.024	25.026	25.5615
Rflns measd	13874	44515	42635
Unique data	6090	13690	14755
R_{int}	0.0937	0.0662	0.0589
wR2[b]	0.1912	0.1729	0.1077
R1[c]	0.0982	0.0680	0.0544
GoF[a]	1.135	1.060	1.101
CCDC number	1864092	1864093	1864094

For $I > 2\sigma(I)$: [a] $R_1 = \Sigma||F_o|-|F_c||/\Sigma|F_o|$. [b] $wR_2 = [\Sigma[w(F_o^2-F_c^2)^2]/\Sigma[w(F_o^2)^2]]^{½}$. [c] Goodness-of-fit $[\Sigma[w(F_o^2-F_c^2)^2]/(N_{obs}-N_{params})]^{½}$.

Table S2 : Crystallographic Data for **1**^{Cy}, **2**^{Cy}, **4**

	1^{Cy}	**2**^{Cy}	**4**
Formula	$C_{55}H_{65}Cl_2N_2P_3Ru$	$C_{55}H_{64}ClN_2P_3Ru$	$C_{55}H_{46}ClN_2P_3Ru, {}_{1.5}(C_6\ H_6)$
Mw	1018.97	982.51	1081.53
Space group	P -1	P 2_1/c	P2_1/c
V (Å^3)	2968.5(4)	6018.9(2)	5299.4(5)
a (Å)	11.854(1)	12.164(1)	15.919(1)
b (Å)	14.926(1)	30.321(1)	14.857(1)
c (Å)	19.142(1)	16.583(1)	23.059(1)
α (deg)	69.988(1)	90	90
β (deg)	82.727(1)	100.227(1)	103.659(1)
γ (deg)	68.875(1)	90	90
Z	2	4	4
d (g.cm^{-3})	1.140	1.084	1.356
F(000)	1064	2056	2236
θ_{max}	27.482	25.025	27.483
Rflns measd	41532	60406	38001
Unique data	13490	10375	12040
R_{int}	0.0595	0.0343	0.0550
wR2[b]	0.1009	0.1222	0.0927
R1[c]	0.0505	0.0619	0.0488
GoF[a]	1.080	1.136	1.056
CCDC number	1864095	1864096	1864097

For $I > 2\sigma(I)$: [a] $R_1 = \Sigma||F_o|-|F_c||/\Sigma|F_o|$. [b] $wR_2 = [\Sigma[w(F_o^2-F_c^2)^2]/\Sigma[w(F_o^2)^2]]^{½}$. [c] Goodness-of-fit $[\Sigma[w(F_o^2-F_c^2)^2]/(N_{obs}-N_{params})]^{½}$.

Table S3 : Crystallographic Data for **3**^{Cy}.

	3^{Cy}
Formula	$C_{55}H_{66}ClN_2P_3Ru$
Mw	984.52
Space group	P 2_1/n
V (Å^3)	10195.6(3)
a (Å)	25.7223(5)
b (Å)	12.2413(2)
c (Å)	32.4835(6)
α (deg)	90
β (deg)	94.5770(5)
γ (deg)	90
Z	8
d (g.cm^{-3})	1.283
F(000)	4128
θ_{max}	27.482
Rflns measd	62437
Unique data	22790
wR2[b]	0.0427
R1[c]	0.1587
GoF[a]	0.0656
GoF	1.183
CCDC number	1864098

For $I > 2\sigma(I)$: [a] $R_1 = \Sigma||F_o|-|F_c||/\Sigma|F_o|$. [b] $wR_2 = [\Sigma[w(F_o^2-F_c^2)^2]/\Sigma[w(F_o^2)^2]]^{½}$. [c] Goodness-of-fit $[\Sigma[w(F_o^2-F_c^2)^2]/(N_{obs}-N_{params})]^{½}$.

II. NMR spectra

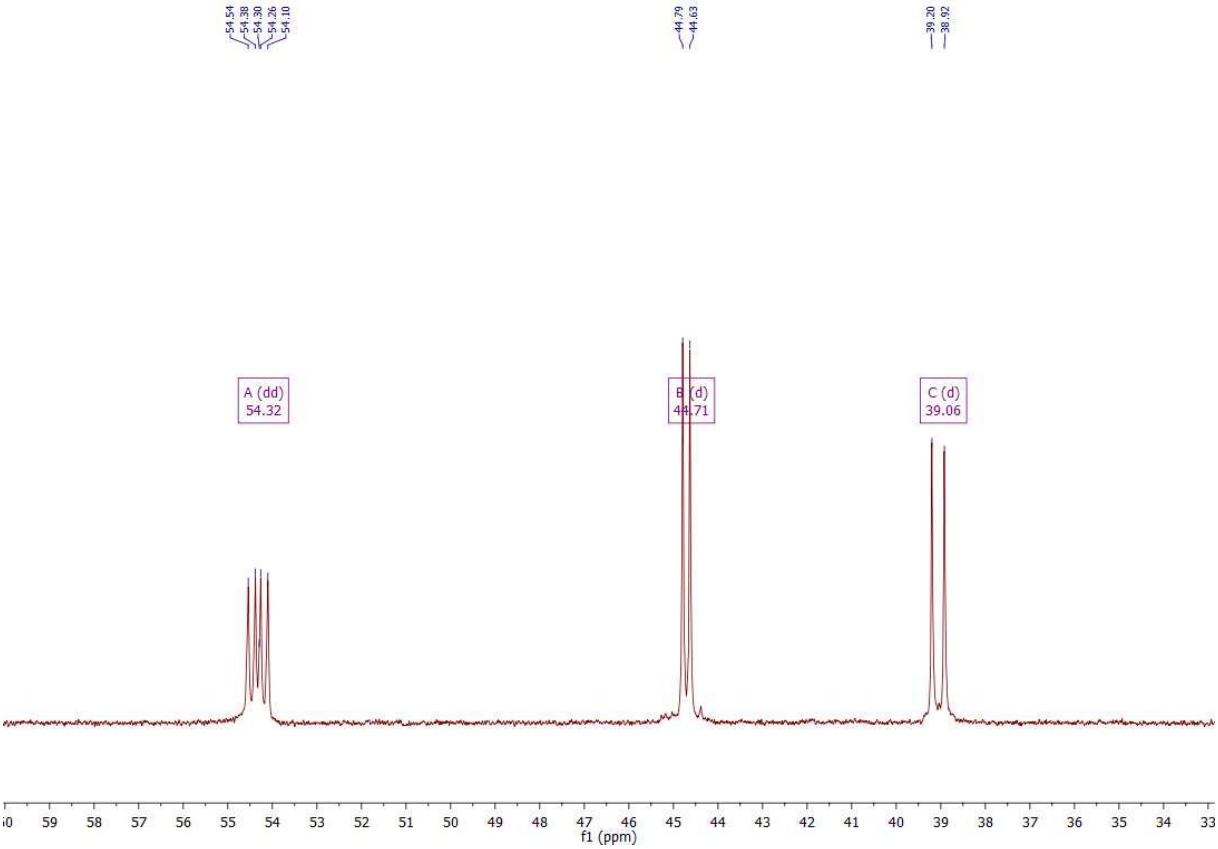

Figure S1: $^{31}P\{^{1}H\}$ NMR spectrum of $\mathbf{1^{Ph}}$ in benzene.

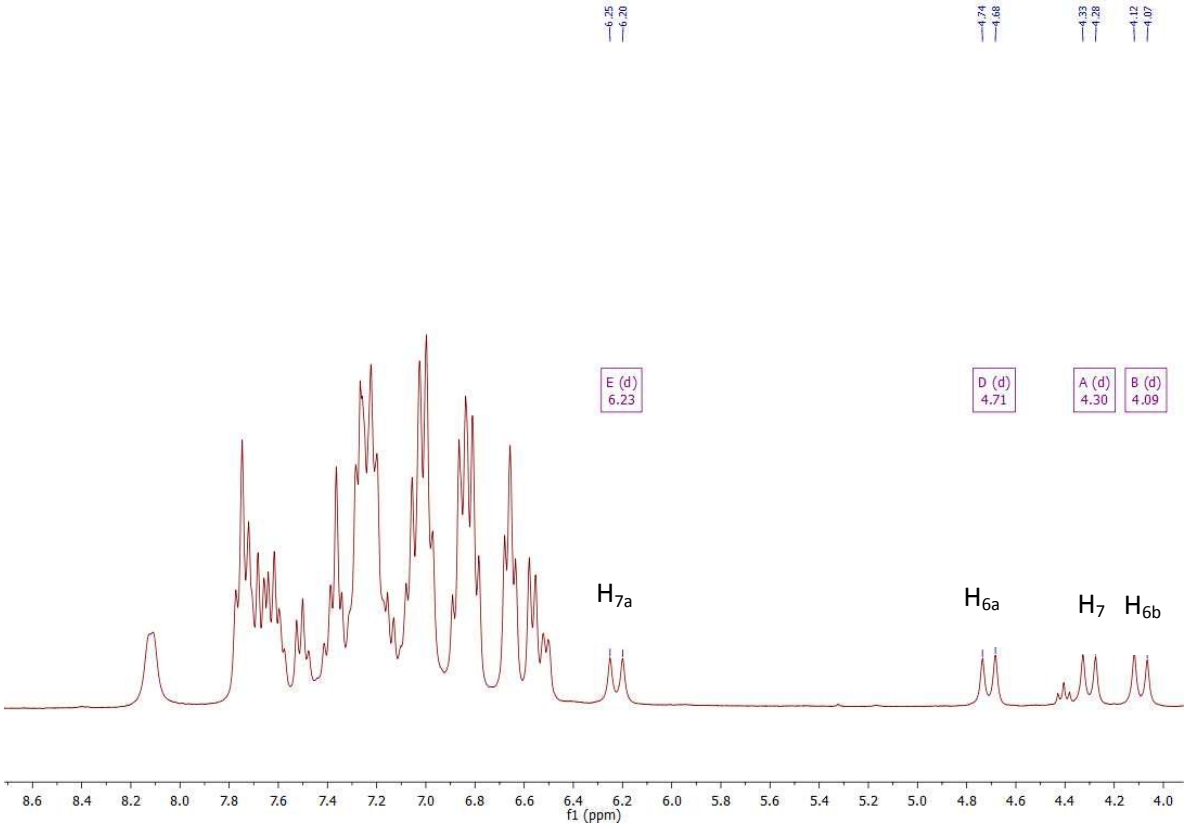

Figure S2: $^{1}H\{^{31}P\}$ NMR spectrum of $\mathbf{1^{Ph}}$ in $CDCl_3$ at -60 °C.

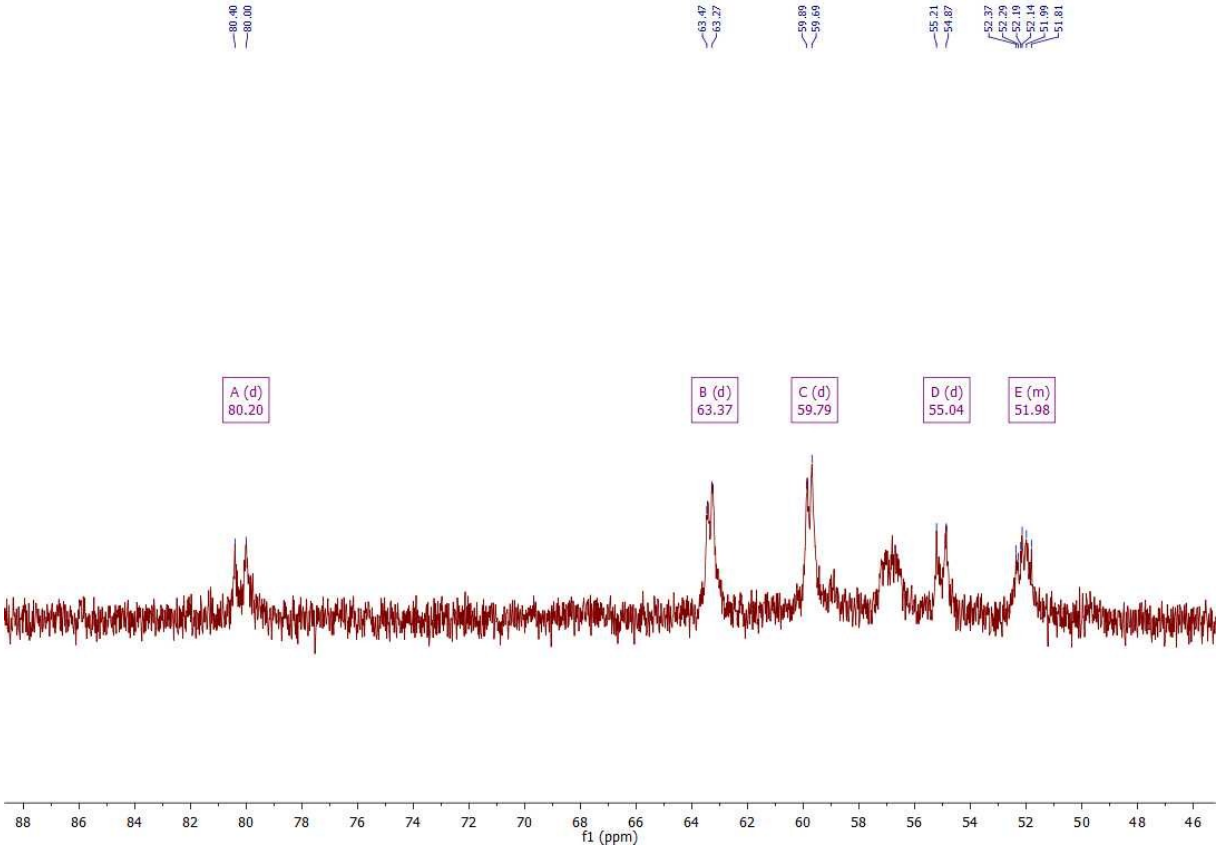

Figure S3 : $^{31}P\{^{1}H\}$ NMR spectrum of $\mathbf{1^{Cy}}$ in CD_2Cl_2.

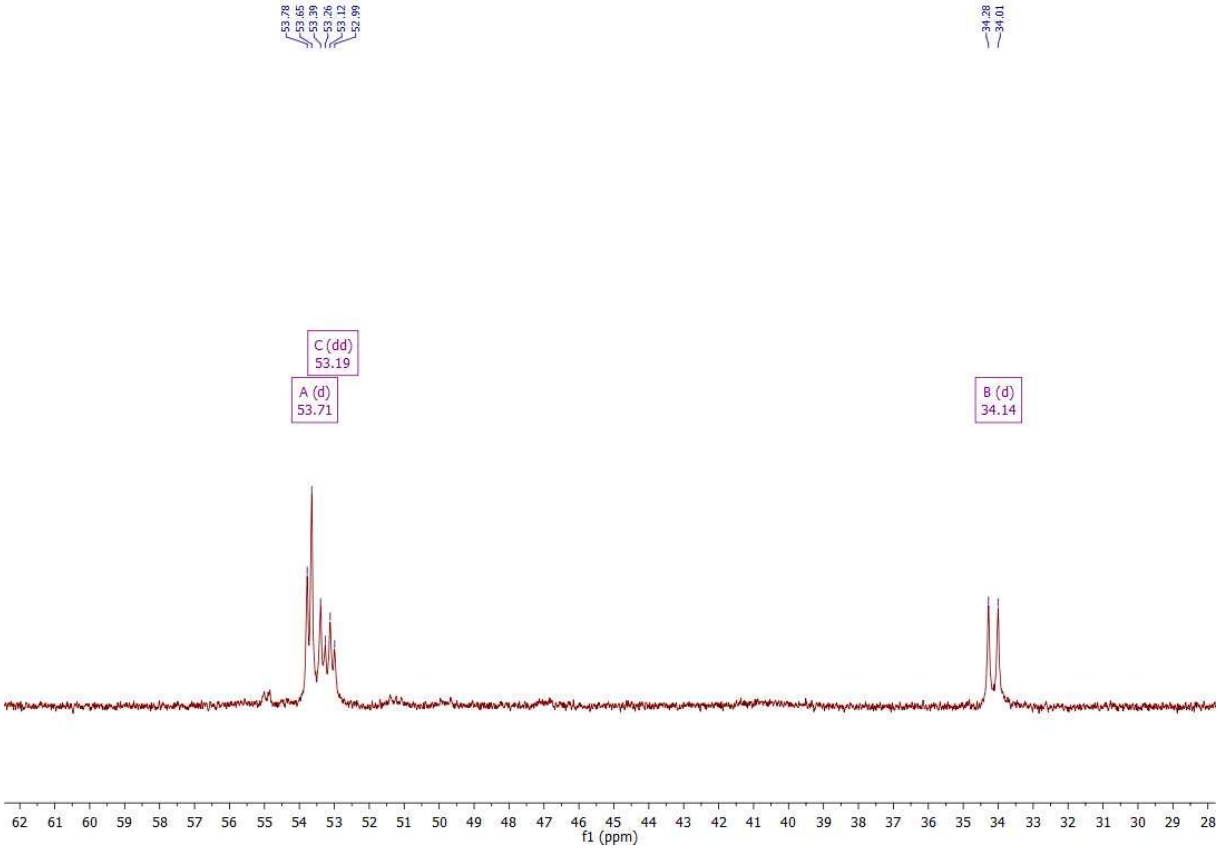

Figure S4: $^{31}P\{^{1}H\}$ NMR spectrum of $\mathbf{1^{Cy}}$ in toluene.

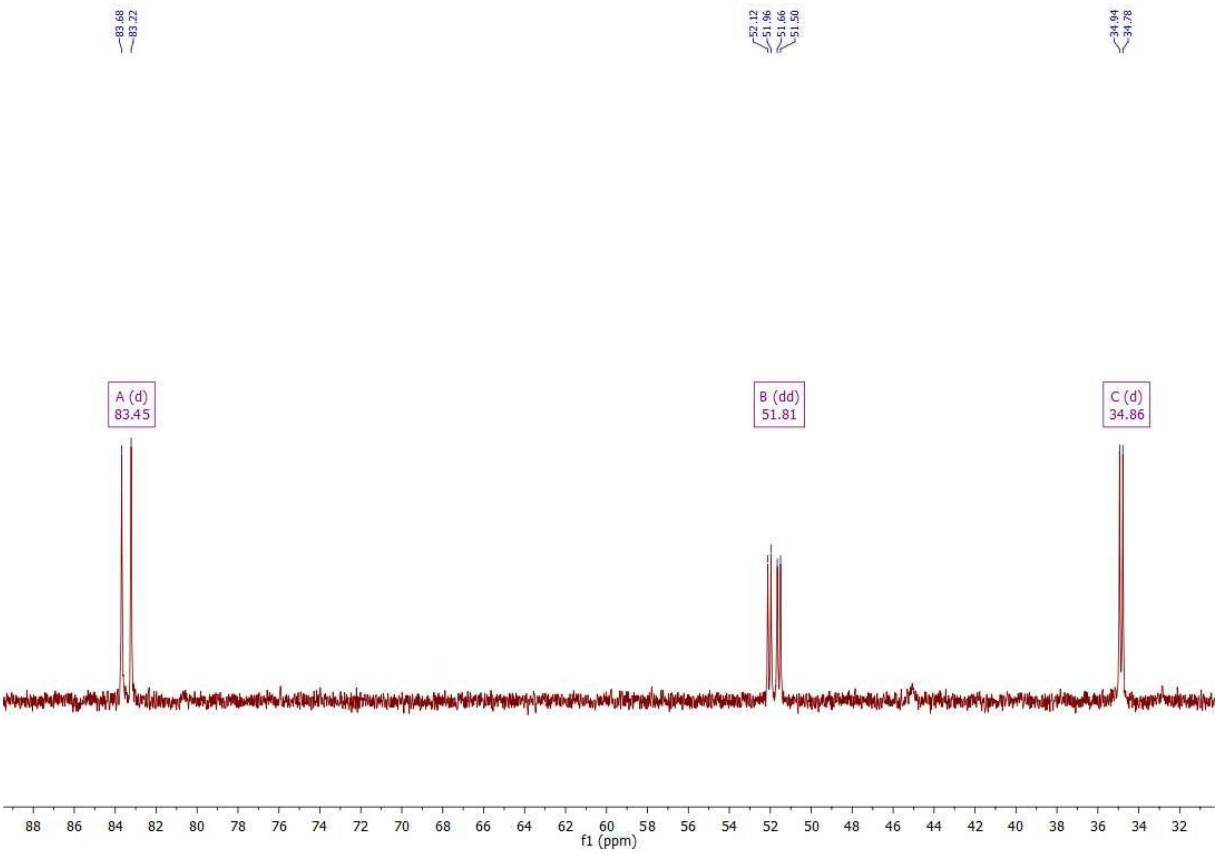

Figure S5: $^{31}P\{^{1}H\}$ NMR spectrum of **2^{Ph}** in benzene.

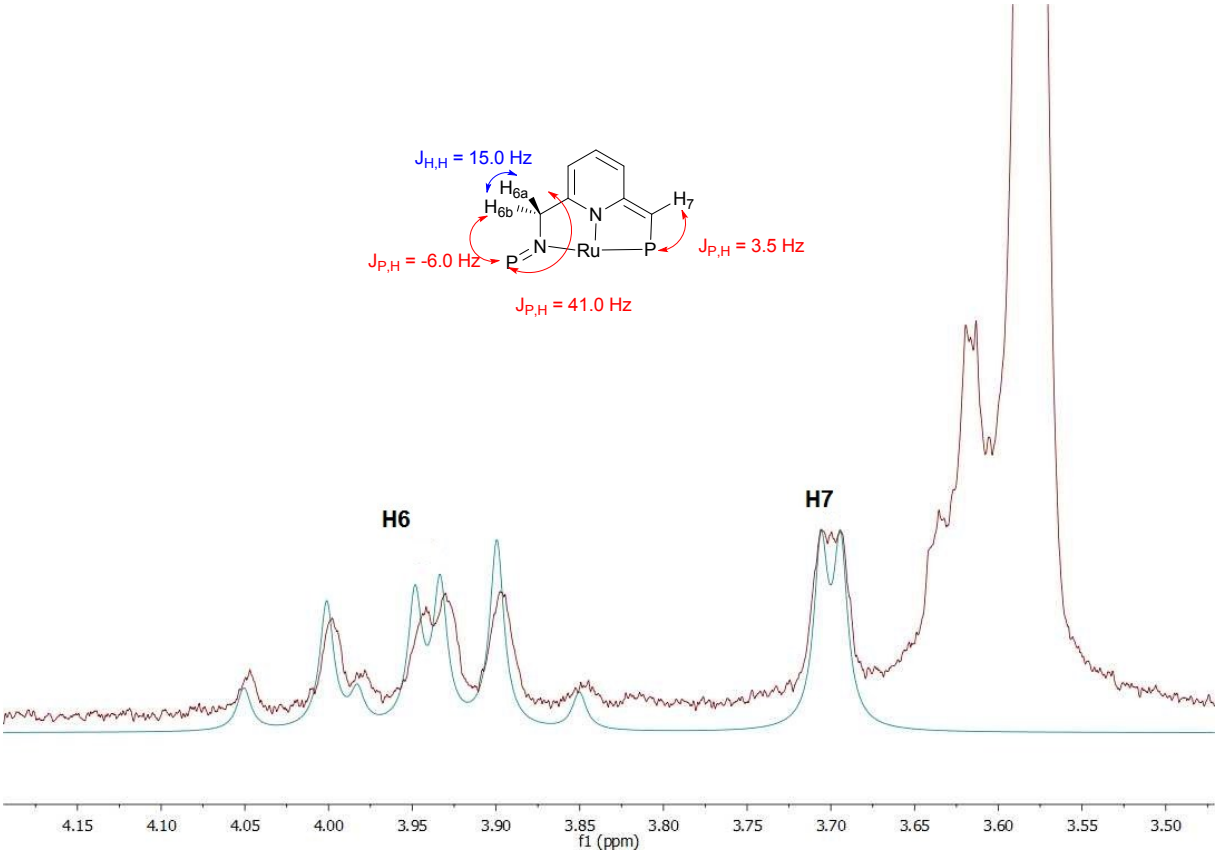

Figure S6: Overlay of experimental (brown) and simulated (teal) ^{1}H NMR spectrum of **2^{Ph}** in THF-d_8 (centered on the benzylic proton region). Coupling constants used to simulate the ABX pattern of H6 are indicated in the inset, $\delta_{H6a} = 3.94$ and $\delta_{H6a} = 3.95$ ppm.

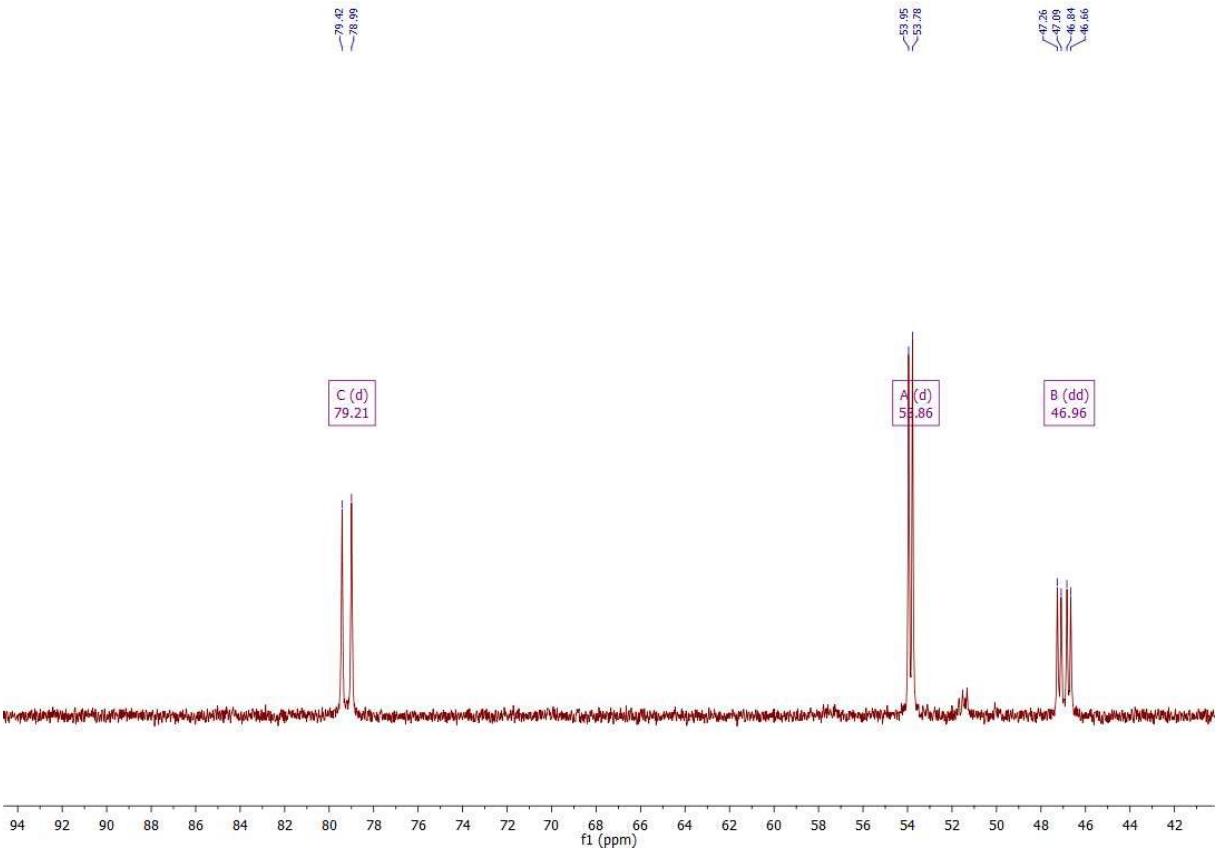

Figure S7: $^{31}P\{^{1}H\}$ NMR spectrum of $\mathbf{2^{Cy}}$ in benzene

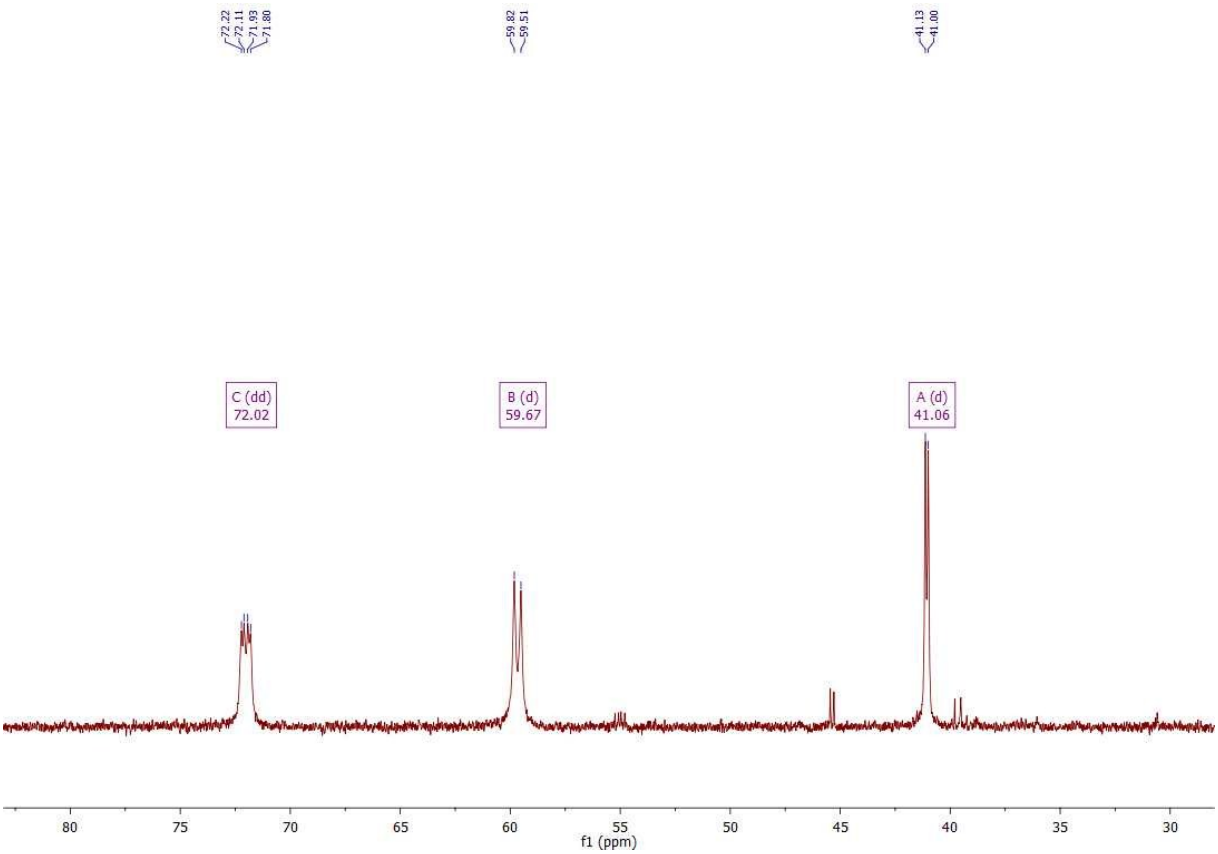

Figure S8: In-situ $^{31}P\{^{1}H\}$ NMR spectrum of $\mathbf{3^{Ph}}$ in benzene.

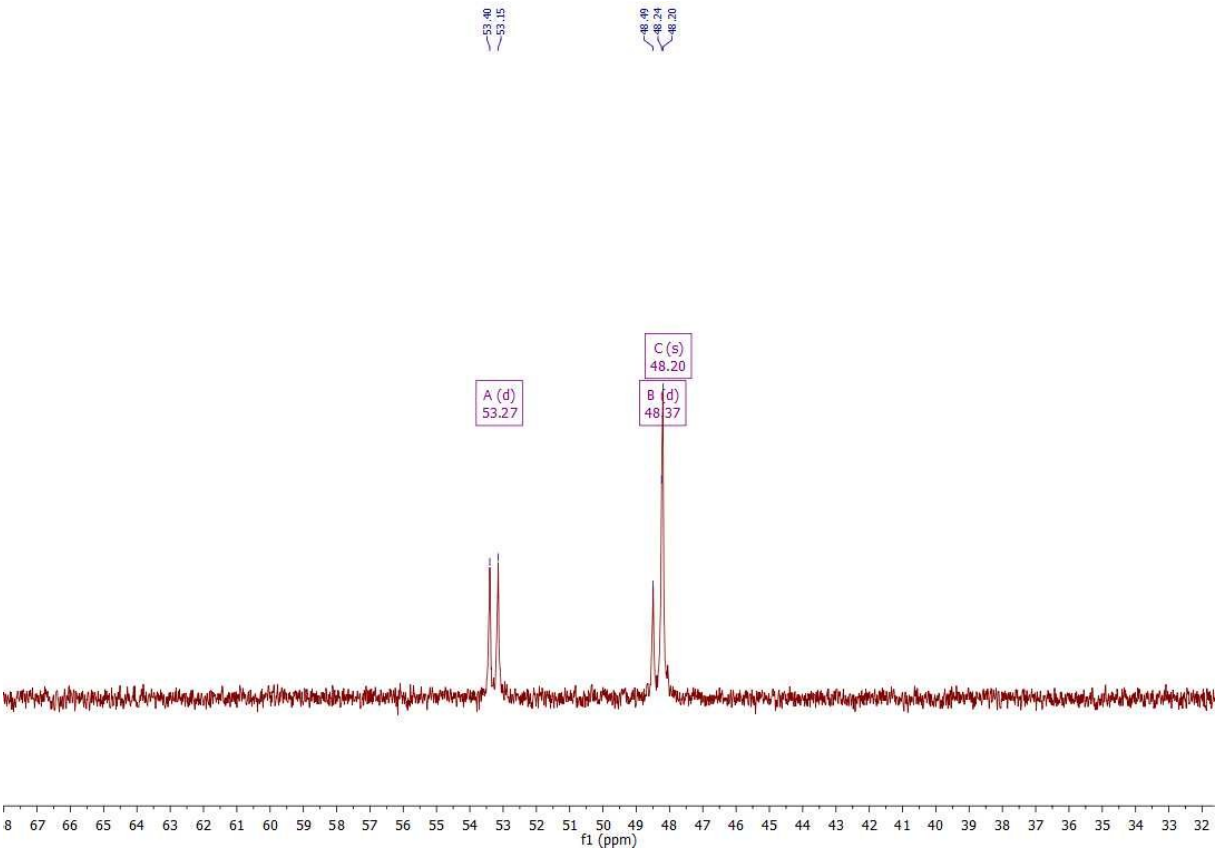

Figure S9: $^{31}P\{^{1}H\}$ NMR spectrum of **4** in toluene-d_8.

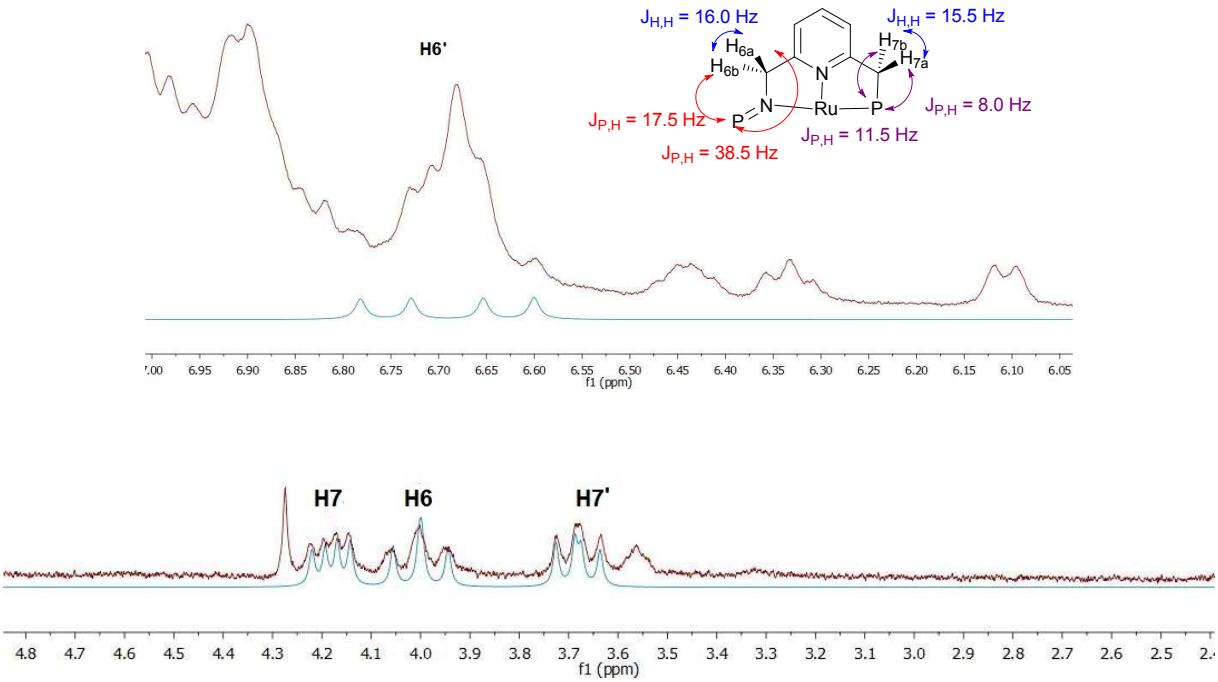

Figure S10: Overlay of experimental (brown) and simulated (teal) ^{1}H NMR spectrum of **4** in C_6D_6. Coupling constants used to simulate the AMX patterns of H_6 and H_7 are indicated in the inset.

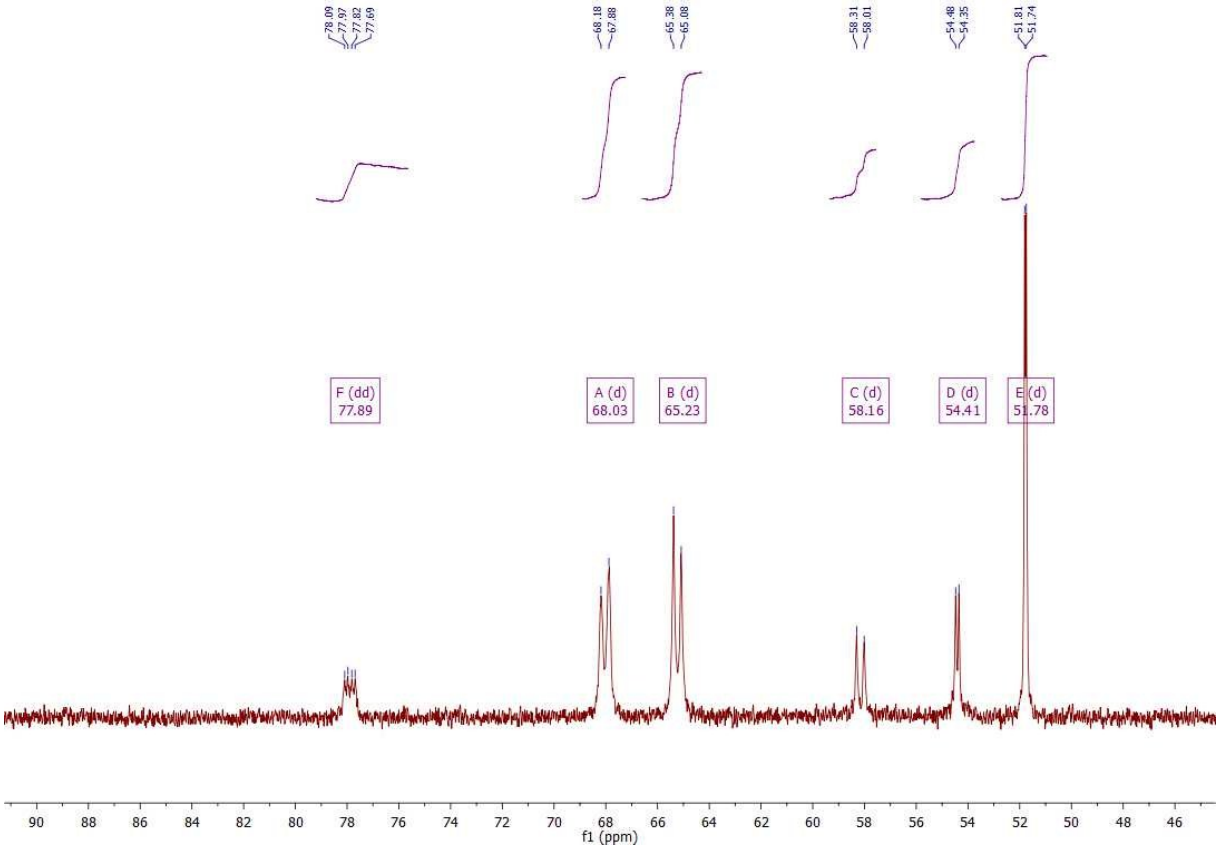

Figure S11: $^{31}P\{^{1}H\}$ NMR spectrum of $\mathbf{3^{Cy}}$ in THF-d_8.

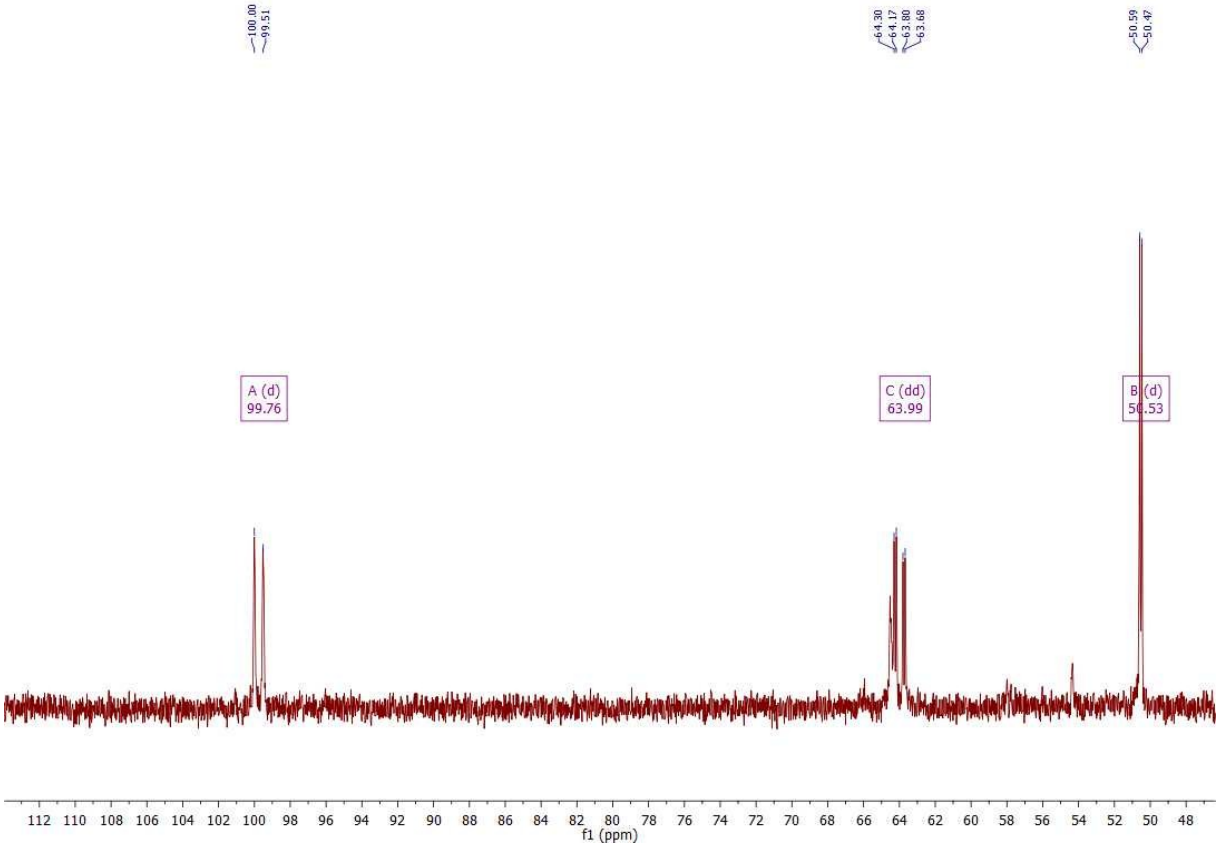

Figure S12: $^{31}P\{^{1}H\}$ NMR spectrum of **5** in THF-d_8.

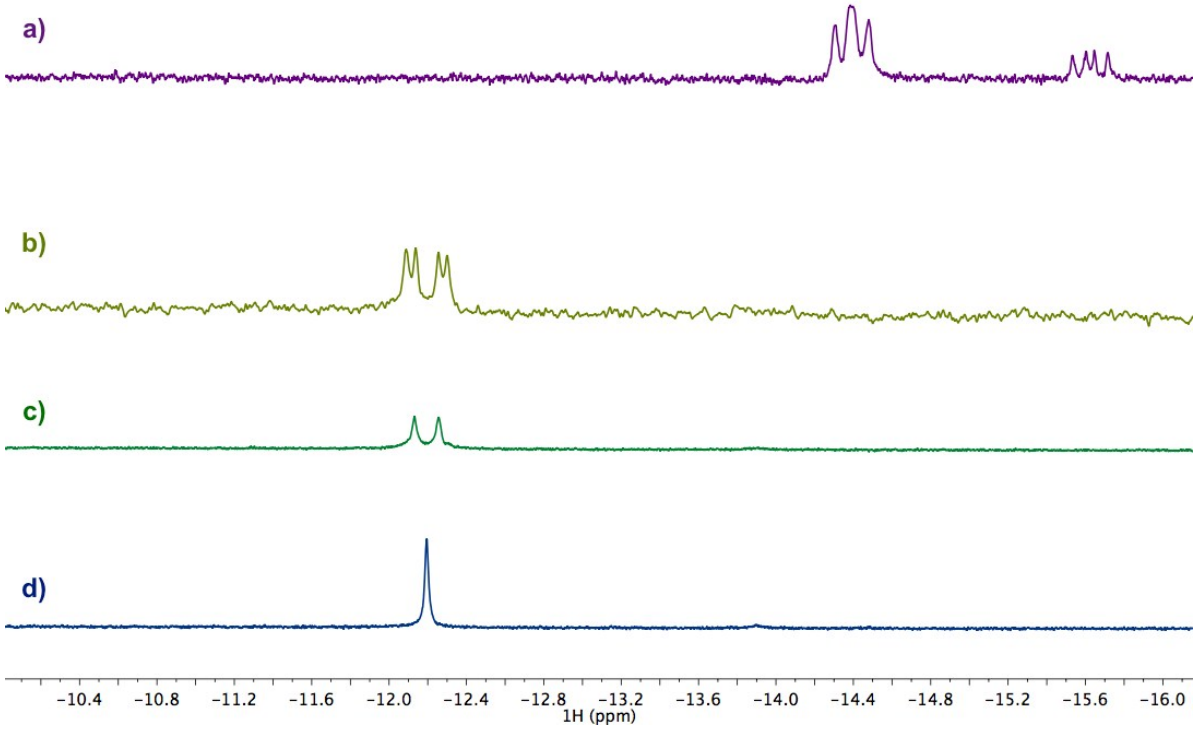

Figure S13: ^{1}H NMR (in THF-d_8) hydride resonances of: a) **3**^{Cy} (2 isomers); b) **5** (no ^{31}P decoupling); c) **5** (with ^{31}P decoupling at 100 ppm); d) **5** (full ^{31}P decoupling).